

# Photochemistry of Roussin's Red Salt, $\text{Na}_2[\text{Fe}_2\text{S}_2(\text{NO})_4]$ , and of Roussin's Black Salt, $\text{NH}_4[\text{Fe}_4\text{S}_3(\text{NO})_7]$ . *In Situ* Nitric Oxide Generation To Sensitize $\gamma$ -Radiation Induced Cell Death<sup>1</sup>

James Bourassa,<sup>2a</sup> William DeGraff,<sup>2b</sup> Setsuko Kudo,<sup>2a</sup> David A. Wink,<sup>2b</sup>  
James B. Mitchell,<sup>2b</sup> and Peter C. Ford<sup>\*,2a</sup>

Contribution from the Department of Chemistry, University of California, Santa Barbara, California 93106, and Radiation Biology Branch, National Cancer Institute, National Institutes of Health, Bethesda, Maryland 20892

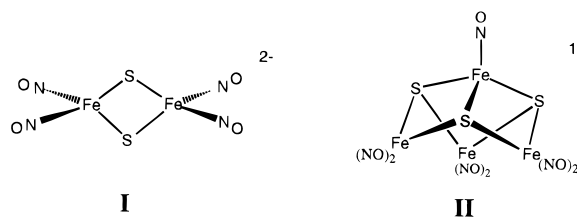
Received November 12, 1996<sup>⊗</sup>

**Abstract:** The quantitative photoreactivities in solution of Roussin's red salt (RRS,  $\text{Na}_2[\text{Fe}_2\text{S}_2(\text{NO})_4]$ ) and of Roussin's black salt (RBS,  $\text{NH}_4[\text{Fe}_4\text{S}_3(\text{NO})_7]$ ) are described. Photolysis of the red Roussinate anion  $\text{Fe}_2\text{S}_2(\text{NO})_4^{2-}$  in aerobic aqueous solution leads to quantitative formation of the black Roussinate anion  $\text{Fe}_4\text{S}_3(\text{NO})_7^-$ . The quantum yield for disappearance of  $\text{Fe}_2\text{S}_2(\text{NO})_4^{2-}$  ( $\Phi_{\text{I}} = 0.14$ ) is independent of excitation wavelength over a broad range (313–546 nm). Real time detection of nitric oxide by electrochemical sensors in the photolysis solution demonstrated the release of NO with a quantum yield of 0.07. The black Roussinate anion is much less photoactive ( $\Phi_{\text{II}} = 1.1 \times 10^{-3}$ ) but does undergo photodecomposition in aerobic solution to give, eventually, ferric precipitates plus NO. These studies were initiated with the goal of developing photochemical strategies for delivering NO to biological targets on demand. In this context, the photolability of  $\text{Fe}_2\text{S}_2(\text{NO})_4^{2-}$  was examined as a possible candidate for exploiting the known nitric oxide sensitization of  $\gamma$ -radiation induced cell killing in V79 cell cultures (Mitchell, J. B.; et al. *Cancer Res.* **1993**, *53*, 5845–5848). Hypoxic cell cultures treated with RRS solution (1.0 mM) and then subjected to  $\gamma$ -radiation (15 Gy) demonstrated strikingly lower survival rates when simultaneously exposed to white light irradiation than did control systems treated identically but in the dark. The black salt was similarly probed, but its greater toxicity and lower quantum yields for NO release make this a less likely candidate for such photochemically induced radiation sensitization.

## Introduction

The discoveries that nitric oxide serves important roles in mammalian bioregulation and immunology<sup>3</sup> have stimulated intense interest in the chemistry and biochemistry of NO and its derivatives such as metallo nitrosyl complexes. Also of interest are precursor compounds which can serve to deliver NO to biological targets on demand.<sup>4</sup> For example, a problem of serious concern in the radiotherapy of malignant tumors is the presence of hypoxic (oxygen deficient) locales within the tumor. Since hypoxic cells are much more resistant to ionizing radiation than are aerobic cells, a goal of radiation biology is to identify new approaches for the sensitization of these to radiation.<sup>5</sup> Reports that nitric oxide delivered as a gas<sup>6</sup> or by

the thermochemical reaction of a NO precursor<sup>7,8</sup> sensitizes the radiation-induced mortality of hypoxic cell cultures indicate the desirability of a viable strategy for NO delivery to specific targets. One such strategy would be to employ a precursor which displays relatively low thermal reactivity but is photochemically active to give NO when subjected to electronic excitation. This proposition led the authors to investigate photochemical properties of iron–sulfur–nitrosyl cluster anions of the type  $\text{Fe}_x\text{S}_y(\text{NO})_z^{n-}$  first reported by Roussin in 1858,<sup>9</sup> specifically, Roussin's red salt (RRS,  $\text{Na}_2[\text{Fe}_2\text{S}_2(\text{NO})_4]$ ) and Roussin's black salt (RBS,  $\text{NH}_4[\text{Fe}_4\text{S}_3(\text{NO})_7]$ ), the anions of which are represented as **I** and **II**.<sup>10</sup> Also described are attempts to use the photochemistries of **I** and **II** as vehicles for delivering NO to hypoxic cell cultures in order to sensitize radiation damage.



The water soluble Roussin's salts were chosen for this study not only because they carry numerous NO equivalents but also

<sup>⊗</sup> Abstract published in *Advance ACS Abstracts*, March 1, 1997.

(1) Preliminary reports presented March 1995 at the 43rd Annual Meeting of the Radiation Research Society, San Jose, CA, Abstract S12–1; April 1995 at the 209th National Meeting of the American Chemical Society, Anaheim, CA, Abstract INOR 355; and March 1996 at the 211th National Meeting of the American Chemical Society, New Orleans, LA, Abstract INOR 626.

(2) (a) University of California, Santa Barbara. (b) Radiation Biology Branch, National Cancer Institute.

(3) (a) Moncada, S.; Palmer, R. M. J.; Higgs, E. A. *Pharmacol. Rev.* **1991**, *43*, 109–142. (b) Furchgott, R. F.; Vanhoutte, P. M. *FASEB J.* **1989**, *3*, 2007–2018. (c) Feldman, P. L.; Griffith, O. W.; Stuehr, D. J. *Chem. Eng. News* **1993**, *71* (10), 26–38. (d) Wink, D. A.; Hanbauer, I.; Grisham, M. B.; Laval, F.; Nims, R. W.; Laval, J.; Cook, J.; Pacelli, R.; Liebmann, J.; Krishna, M.; Ford, P. C.; Mitchell, J. B. *Curr. Top. Cell. Regul.* **1996**, *34*, 159–187 and references therein. (e) Feelish, M.; Stamler, J. S., Eds. *Methods in Nitric Oxide Research*; J. Wiley and Sons: Chichester, England, 1996 and references therein.

(4) Feelish, M.; Stamler, J. S. Ref 3e, Chapter 7, pp 71–113.

(5) Hall, E. J. *Radiobiology for the Radiologist*; J. B. Lippincott Co.: Philadelphia, 1988.

(6) Howard-Flanders, P. *Nature (London)* **1957**, *180*, 1191–1192.

(7) Mitchell, J. B.; Wink, D. A.; DeGraff, W.; Gamson, J.; Keefer, L. K.; Krishna, M. C. *Cancer Res.* **1993**, *53*, 5845–5848.

(8) Griffin, R. J.; Song, C. W. Presented at the 43rd Annual Meeting of the Radiation Research Society, San Jose, CA, April 1995; Abstract P15–204.

(9) Roussin, M. L. *Ann. Chim. Phys.* **1858**, *52*, 285.

(10) Butler, A. R.; Glidewell, C.; Li, M.-H. *Adv. Inorg. Chem.* **1988**, *32*, 335.

because their optical spectra have high absorptivities even into the red, a feature attractive for possible use in tissues. The black Roussinate anion,  $\text{Fe}_4\text{S}_3(\text{NO})_7^-$ , has been the subject of several studies with vascular and brain tissues as a drug for the thermochemical or photochemical delivery of  $\text{NO}$ ,<sup>11,12</sup> indeed, a biological assay (rat tail artery relaxation) was used to demonstrate the  $\text{NO}$  release upon RBS photolysis in buffer solutions.<sup>11b</sup> RBS has also received attention owing to its very potent bacteriostatic properties,<sup>13,14</sup> and it has been argued that treating meat products with nitrite salts may lead to the formation of **II**, which inhibits bacterial growth. The red Roussin's salt has primarily been studied as a synthetic precursor.<sup>15</sup> The quantitative photochemistry of these systems has received little attention.

The quantitative photoreaction studies described here demonstrate that the red Roussinate anion  $\text{Fe}_2\text{S}_2(\text{NO})_4^{2-}$  undergoes photoconversion to the black anion **II** with no other detectable  $\text{Fe-S-NO}$  products and that  $\text{Fe}_4\text{S}_3(\text{NO})_7^-$  undergoes net photochemistry (but only in oxygenated solutions) first to form ferrous ions and then to give ferric precipitates. Real time, quantitative detection of the  $\text{NO}$  labilized from both anions was performed during photolyses using electrochemical sensors. Also described are effects on the mortalities of hypoxic V79 Chinese hamster lung cells treated with RRS or RBS and then exposed to visible light, to  $\gamma$ -radiation, or to combinations of the two. Photolysis of RRS treated systems sensitized the radiation effects, illustrating the viability of photochemical strategies for  $\text{NO}$  delivery to biological targets. However, RBS proved to be quite toxic to these cell cultures.

## Experimental Section

**Materials.** Roussin's red and black salts were prepared as the hydrates  $\text{Na}_2[\text{Fe}_2\text{S}_2(\text{NO})_4] \cdot 8\text{H}_2\text{O}$  and  $\text{NH}_4[\text{Fe}_4\text{S}_3(\text{NO})_7] \cdot \text{H}_2\text{O}$  by literature methods.<sup>15</sup> IR spectra of the solids in KBr displayed  $\nu_{\text{NO}}$  bands at 1717 (s) and 1677 (s)  $\text{cm}^{-1}$  and at 1800 (w), 1745 (vs) and 1715 (s)  $\text{cm}^{-1}$ , respectively.<sup>16</sup> All other compounds used were reagent grade. Organic solvents were distilled from calcium hydride and used promptly, with the exception of DMSO, which was distilled under reduced pressure from sodium and stored over molecular sieves. Nitric oxide gas was obtained from Matheson and passed through an Ascarite scrubber before use. Nitrous oxide was obtained as a 10% mixture with helium from Aldrich. Aqueous  $\text{NO}$  solutions were prepared by stirring nanopure water, which had been deaerated by a sequence of five freeze-pump-thaw cycles, under appropriate  $P_{\text{NO}}$  for 2 h and

were standardized spectroscopically using the oxymyoglobin method.<sup>17</sup> Sodium phosphate buffers were used to prepare solutions in the pH range 6–8, sodium borate buffers for higher pH and salicylic acid solutions for lower pH.

**Instruments.** Infrared spectra were obtained with a BioRad FTS 60 SPC 3200 FTIR spectrometer. UV-vis absorption spectra were obtained with either a HP8572 diode array or a Cary 118 spectrophotometer modernized by OLIS. Gas chromatography was carried out using a 5830A gas chromatograph with a 12 ft 80/100 Porapak Q column at 140 °C.  $\text{NO}$  retention times were similar to those of  $\text{N}_2$ , appearing at 1.27 min after injection, while  $\text{N}_2\text{O}$  appeared 2.07 min after injection.

**Photolysis Experiments.** UV-vis absorption spectra and photolysis experiments under deaerated conditions were carried out in 1 cm quartz cells fitted with glass stopcocks via Viton O-ring joints. Deaeration of solutions was achieved with 3–5 freeze-pump-thaw (f-p-t) cycles. Continuous photolysis experiments were performed on optical trains using UVP 200 W Hg lamps and the appropriate interference filters as the excitation source.<sup>18</sup> Chemical actinometry was performed with ferric oxalate solutions for  $\lambda_{\text{irr}} < 450$  nm and with Reinecke salt solutions for longer wavelengths.<sup>19</sup> A separate photolysis train was assembled to use in experiments for electrochemical detection of  $\text{NO}$ .<sup>20</sup> Preliminary flash photolysis experiments were carried out with a time-resolved optical (TRO) apparatus using the third harmonic (355 nm) of a Nd:YAG nanosecond pulse laser (Continuum NY60-20) as the pump source.<sup>21</sup> The probe source was a high-pressure short-arc xenon lamp, and time-resolved detection was effected either with a SPEX Doublemate monochromator and RCA Model 8852 photomultiplier tube (monochromatic) or with an Acton Research Corp. SpectraPro-275 spectrograph and a Princeton LN2 cooled CCD camera (broad band).

**Electrochemical NO Detection.** The  $\text{NO}$  sensors used were of three types. Qualitative detection of photochemical release in RRS solutions was first accomplished using a carbon fiber (CF) microelectrode (Medical Systems) which had been modified by electropolymerization of a nickel porphyrin and then coated with Nafion.<sup>22</sup> Quantitative measurements were made using two combination electrode  $\text{NO}$  sensors. One was custom built with a modified glassy carbon (GC) disk working electrode, a silver wire quasireference electrode, and an oxygen sensor type Teflon membrane.<sup>20</sup> The other was a World Precision Instruments (WPI) Model ISO-NOP electrode adapted for use with a BAS-100B electrochemical analyzer. The oxidation of  $\text{NO}$  on these sensors was observed typically at 650 mV vs SCE, and the monitoring potential was kept 100 mV above the  $\text{NO}$  oxidation peak center. Nitrous oxide, sulfide, and the Roussinate salts were tested for possible electrochemical interference, but gave minimal signals upon injection into the photolysis media. Nitrite ion interference was minimized by the Nafion coatings and was checked for every newly prepared sensor (e.g., for one modified GC electrode,  $\text{NO}_2^-$  showed a sensitivity of  $\sim 3$  nA/mM compared to  $\text{NO}$  sensitivity of  $\sim 22$  nA/ $\mu\text{M}$ ).

Photolyses were carried out in 3 cm diameter cylindrical Pyrex cells. A 10 mL volume of the Roussinate solution would be pipetted into the cells, and the electrochemical sensor would be immediately calibrated by injection of a known quantity of  $\text{NO}$  stock solution. Photolysis was then initiated and the signal due to  $\text{NO}$  formation recorded in real time. The UV-vis spectra of the solutions were recorded immediately

(11) (a) Flitney, F. W.; Megson, I. L.; Flitney, D. E.; Butler, A. R. *Br. J. Pharmacol.* **1992**, *107*, 842–848. (b) Flitney, F. W.; Megson, I. L.; Thomson, J. L. M.; Kennovin, G. D.; Butler, A. R. *Br. J. Pharmacol.* **1996**, *117*, 1549–1557.

(12) Matthews, E. K.; Seaton, E. D.; Forsyth, M. J.; Humphrey, P. P. A. *Br. J. Pharmacol.* **1994**, *113*, 87–94.

(13) (a) Moran, D. J.; Tannenbaum, S. R.; Archer, M. C. *Appl. Microbiol.* **1975**, *30*, 838–843. (b) Maraj, S. R.; Khan, S.; Cui, X.-Y.; Cammack, R.; Joannou, C. L.; Hughes, M. N. *Analyst* **1995**, *120*, 699–703.

(14) (a) Ashworth, J.; Didcock, A.; Hargreaves, L. L.; Jarvis, B.; Walters, C. L. *J. Gen. Microbiol.* **1974**, *84*, 403–408. (b) Payne, M. J.; Glidewell, C.; Cammack, R. *J. Gen. Microbiol.* **1990**, *136*, 2077–2087. (c) Ryu, J.-S.; Lloyd, D. *FEMS Microbiol. Lett.* **1995**, *130*, 183–188.

(15) (a) Rauchfuss, T. B.; Weatherill, T. D. *Inorg Chem.* **1982**, *21*, 827–830. (b) Seyferth, D.; Gallagher, M. K.; Cowie, M. *Organometallics* **1986**, *5*, 539–548. (c) Brauer, G., Ed.; *Handbook of Preparative Inorganic Chemistry*, 2nd ed.; Academic Press: New York, 1963; pp 1763–1764.

(16) (a) The IR spectrum of the RBS agrees well with that published by Chu and Dahl.<sup>16b</sup> For the dinuclear red salt, the IR spectrum of the sodium salt of **I** displays a pattern of  $\nu_{\text{NO}}$  bands nearly identical to that of the published spectrum of the  $\text{AsPh}_4^+$  (1660 and 1618  $\text{cm}^{-1}$ )<sup>16c</sup> but shifted to higher frequency. Precipitation of **I** by addition of  $\text{AsPh}_4^+$  to a solution of the sodium salt in water gives a material with an IR spectrum identical to that published, so the shifts appear to be the result of specific cation interactions with the cluster anion in the solid. (b) Chu, C. T.-W.; Dahl, L. F. *Inorg. Chem.* **1977**, *16*, 3245–3251. (c) Beck, W.; Grenz, R.; Gotzfried, F.; Vilsmaier, E. *Chem. Ber.* **1981**, *114*, 3184–3187.

(17) Nims, R. W.; Darbyshire, J. F.; Saavedra, J. E.; Christodoulou, D.; Hanbauer, I.; Cox, G. W.; Grisham, M. B.; Laval, F.; Cook, J. A.; Krishna, M. C.; Wink, D. A. *Methods: Companion Methods Enzymol.* **1995**, *7*, 48–54.

(18) (a) Hintze, R.; Ford, P. C. *J. Am. Chem. Soc.* **1975**, *97*, 2664–2671. (b) Friedman, A. E.; Ford, P. C. *J. Am. Chem. Soc.* **1989**, *111*, 551–558. (c) Carlos, R. M.; Frink, M. E.; Tfouni, E.; Ford, P. C. *Inorg. Chim. Acta* **1992**, *193*, 159–165. (d) Boese, W. T.; Ford, P. C. *J. Am. Chem. Soc.* **1995**, *117*, 8381–8391.

(19) (a) Calvert, J. G.; Pitts, J. N. *Photochemistry*; J. Wiley & Sons: New York, 1967; pp 783–786. (b) Malouf, G.; Ford, P. C. *J. Am. Chem. Soc.* **1977**, *99*, 7213–7221.

(20) Kudo, S.; Bourassa, J.; Boggs, S.; Sato, Y.; Ford, P. *Anal. Biochem.*, in press.

(21) Lindsay, E.; Ford, P. C. *Inorg. Chim. Acta* **1996**, *242*, 51–56.

(22) (a) Malinski, T.; Taha, Z. *Nature (London)* **1992**, *358*, 676. (b) Christodoulou, D.; Kudo, S.; Cook, J. A.; Krishna, M. C.; Miles, A.; Grisham, M. B.; Murugesan, R.; Ford, P. C.; Wink, D. A. *Methods Enzymol.* **1996**, *268*, 69.

before and after photolysis to determine concentration changes of the iron species in solution, and reaction stoichiometries were determined by comparing changes in iron species concentrations with changes in [NO]. Further details will be described elsewhere.<sup>20</sup>

**Electrospray MS Experiments.** Electrospray mass spectroscopy was performed on a VG Fisons Platform II single quadrupole mass spectrometer with an electrospray ionization source by Dr. James Pavlovich of the UC Santa Barbara mass spectrometry facility. Samples were introduced with direct infusion via a Harvard apparatus syringe pump at 20  $\mu\text{L}/\text{min}$  in pure water.

**Cell Culture and Radiation Experiments.** These were carried out at the National Cancer Institute, Radiation Biology Branch, using procedures analogous to those reported previously.<sup>23</sup> Chinese hamster V79 cells were grown in F12 medium supplemented with 10% fetal calf serum, penicillin, and streptomycin. Survival was assessed by the clonogenic assay. The plating efficiency ranged between 80 and 90%. Stock cultures of exponentially growing cells were trypsinized, rinsed, and plated into specially designed 25  $\text{cm}^2$  glass flasks ( $2.0 \times 10^5$  cells/flask in 1.8 mL of medium) and incubated for 16 h at 37  $^\circ\text{C}$  prior to experimental protocols. For experimental procedures under hypoxic conditions, the flasks were sealed with soft rubber stoppers, and 19-gauge needles were pushed through to act as entrance and exit ports for a humidified gas mixture of 95% nitrogen/5%  $\text{CO}_2$  (Matheson Gas Products). Each flask was also equipped with a ground-glass side arm vessel which when rotated and inverted could deliver 0.2 mL of medium containing Roussin's salt at a concentration which when added to the cell monolayer resulted in a final concentration of 500  $\mu\text{M}$ . Stopped flasks were connected in series, mounted on a reciprocating platform, and gassed at 37  $^\circ\text{C}$  for 60 min. This gassing procedure results in an equilibrium between the gas and liquid phase (both in the medium over the cell monolayer and in the solution in the side arm) and yielded oxygen concentrations in the effluent gas phase of <10 ppm as measured by a Thermo probe.<sup>23</sup>

After 60 min of gassing, the deaerated Roussin's salt solution was added to the hypoxic cell monolayer without introducing any air into the flasks by rotating the side arm containing 0.2 mL of a  $10\times$  concentration of the salt. All handling of Roussin's salt solutions and flasks containing these was done under subdued lighting. After addition of the Roussin's salt to the cell monolayer, flasks were immediately illuminated at room temperature (24  $^\circ\text{C}$ ) from below by placing the flasks on a clear plastic stand above a mirror set at a 45 $^\circ$  angle. The plastic stand was mounted below a  $^{60}\text{Co}$  irradiator such that cells could be exposed to light and  $\gamma$ -radiation simultaneously. Light exposure began 2 min prior to the start of  $\gamma$ -radiation and continued for a total of 11 min. Cells treated with Roussin's salt but not exposed to light were exposed to  $\gamma$ -radiation using the same setup as above. The light source was a lantern slide projector ("Slide King", Charles Beseler Co., East Orange, NJ) equipped with a Sylvania 750 W CWA lamp. The lens of the projector was 71 cm from the mirror, producing a uniform light field (100  $\text{cm}^2$  in area) with a maximum intensity of 160  $\text{W}/\text{m}^2$ . A Theratronics Eldorado 8  $^{60}\text{Co}$  irradiator, operating at a dose rate of 2.0 Gy/min was used for cell irradiation. Following treatment, the stoppers were quickly removed and the medium over the cell monolayer was immediately gassed with 95%  $\text{N}_2/5\%$   $\text{CO}_2$  for 2 min. This precaution was taken to prevent autoxidation of gas phase NO, which can form potentially cytotoxic oxides of nitrogen as well as acidify the medium. Cells were then rinsed, trypsinized, counted, and plated for macroscopic colony formation. Each dose determination was plated in triplicate, and experiments were repeated a minimum of two times. Plates were incubated for 7 days, after which colonies were fixed with methanol/acetic acid, stained with crystal violet, and counted. Colonies containing >50 cells were scored. Error bars represent standard deviations of the mean and are shown when larger than the symbol.

## Results

**Photoreactions of Roussin's Black Salt.** The RBS anion **II** is strongly colored with broad absorptions across the UV-vis spectrum. Optical spectrum extinction coefficients exceed  $10^3 \text{ M}^{-1} \text{ cm}^{-1}$  for all  $\lambda < \sim 650 \text{ nm}$  with values at apparent

(23) Russo, A.; Mitchell, J. B.; Finkelstein, E.; DeGraff, W. G.; Spiro, I. J.; Gamson, J. *Radiat. Res.* **1985**, *103*, 232–239.

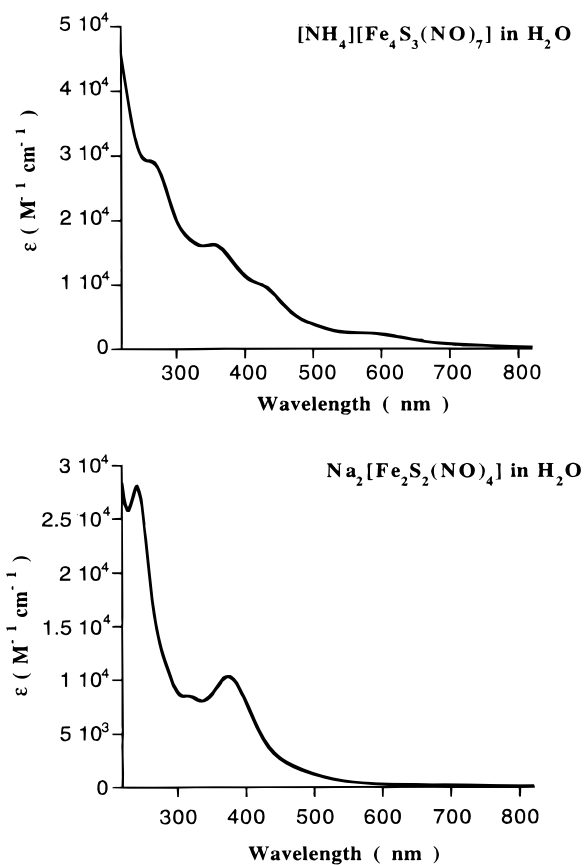


**Figure 1.** Spectra of aqueous solutions of RBS and RRS.

maxima ranging from  $2600 \text{ M}^{-1} \text{ cm}^{-1}$  at 550 nm to  $28\,800 \text{ M}^{-1} \text{ cm}^{-1}$  at 270 nm (Figure 1). According to theoretical calculations on the  $\text{Fe}_4\text{S}_3(\text{NO})_7^-$  anion at the extended Huckel molecular orbital (EHMO) level,<sup>24</sup> these absorptions are primarily transitions between orbitals delocalized over the  $\text{Fe}_4$  cluster, although the LUMO has been characterized as being antibonding with respect to Fe–S and Fe–NO interactions as well as to Fe–Fe bonds.<sup>25</sup>

When carefully deoxygenated aqueous solutions of RBS (pH 7.0 buffered, 296 K) were irradiated at various wavelengths ( $\lambda_{\text{irr}}$ ) throughout the visible region, the electronic spectrum displayed no changes, an observation suggesting the absence of net photochemistry. Similarly, RBS solutions under NO (up to 1 atm) showed no net photochemistry under repetitive pulse laser excitation at 355 nm or continuous (CW) photolysis at 365 nm. However, the situation was different in aerobic solutions, where photolysis at various  $\lambda_{\text{irr}}$  led to decreased optical density across the visible spectrum (Figure 2), and exhaustive photolysis led to formation of an orangish precipitate suggestive of ferric oxides. Aerated RBS solutions in the pH range 6–10 do not undergo measurable spectral changes over a period of hours if kept in the dark,<sup>26</sup> so thermal reaction corrections were not necessary in evaluating the photochemical processes.

**A. Analysis of Products.** The precipitate from the photolysis of an aerobic RBS solution was collected and vacuum dried in an attempt to characterize it. The FTIR spectra of this material in KBr showed strong bands at 1270 and 1385  $\text{cm}^{-1}$

(24) Sung, S.-S.; Glidewell, C.; Butler, A. R.; Hoffmann, R. *Inorg. Chem.* **1985**, *24*, 3856–3859.

(25) D'Addario, S.; Demartin, F.; Grossi, L.; Iapalucci, M. C.; Laschi, F.; Longoni, G.; Zanello, P. *Inorg. Chem.* **1993**, *32*, 1153–1160.

(26) Earlier workers<sup>11b</sup> commented that RBS solutions underwent thermal degradation under the conditions described here; however, we have found little problem with dark reactions while handling these materials during setup and execution of photochemical experiments.

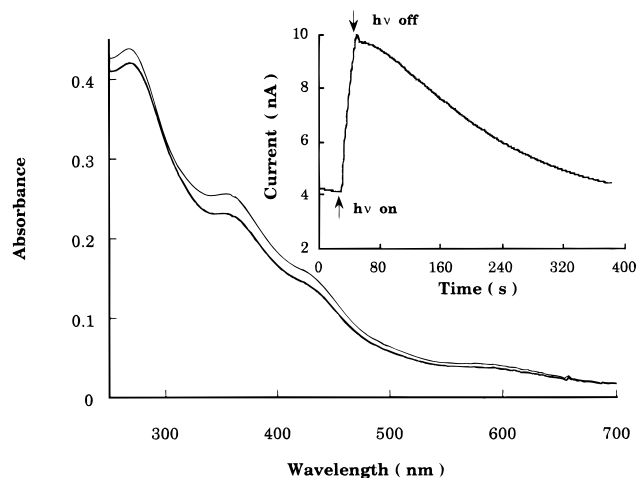


**Figure 2.** Absorption change amperogram of NO released upon white light photolysis of an aerated pH 7.0 phosphate buffered solution of Roussin's black salt. WPI NO sensor used with calibrated sensitivity 0.66 nA/ $\mu\text{M}$ : initial  $[\text{II}] = 15 \mu\text{M}$ ;  $\Delta[\text{II}]$  from spectral changes =  $-1.51 \mu\text{M}$ ;  $\Delta[\text{NO}]$  determined electrochemically =  $9.1 \mu\text{M}$ .

characteristic of  $\text{NO}_2^-$  and  $\text{NO}_3^-$ , respectively.<sup>27</sup> Digesting the precipitate in dilute acid gave a cloudy solution. Addition of sodium thiocyanate solution gave the red color ( $\lambda_{\text{max}} = 480 \text{ nm}$ ) indicating the presence of ferric ion. When the orange RBS photoproduct precipitate was digested in 6 M HCl, the result was a dark yellow solution ( $\lambda_{\text{max}} = 358 \text{ nm}$ ). An identical absorbance could be generated by dissolving  $\text{FeCl}_3$  or  $\text{Fe}(\text{NO}_3)_3$  in 6 M HCl, and this has been attributed to formation of the tetrachloroferrate(III) ion  $\text{FeCl}_4^-$ .<sup>28</sup> Accordingly, a calibration curve was assembled from the absorbances of varied concentrations of  $\text{Fe}(\text{NO}_3)_3$  in 6 M HCl. Different weights of the RBS photoproduct precipitate were then digested in fixed volumes of 6 M HCl, and the resulting absorbances were compared to the calibration curve. In this manner, the vacuum-dried precipitate was determined to be  $45 \pm 2\%$  by weight Fe(III) (four individual determinations).

The residual which was not soluble in 6 M HCl did dissolve in hot toluene. Therefore, separate samples of the RBS photoproduct precipitate were extracted with hot toluene. The resulting extracts were combined and evaporated to dryness, producing light yellow crystals with a melting point of 113–115 °C consistent with the formation of elemental sulfur. After the extraction of sulfur, the precipitate was determined to be 55% Fe by weight. From these two values, the ratio of sulfur to iron, by weight, is 0.40. In the original RBS, the ratio is 0.43.

In order to evaluate the nature of iron species first formed photochemically, aerated aqueous solutions of RBS (15–80  $\mu\text{M}$ ) were photolyzed ( $\lambda_{\text{irr}} = 360\text{--}440 \text{ nm}$ ) for various lengths of time until the decreases in absorptions attributed to **II** were 5–25%. A 1.0 mL aliquot of such a solution was then diluted with a 1.0 mL volume of water, and the UV–vis absorption spectrum was recorded for a base line. Another 1.0 mL aliquot of the photolysis solution was added to a 1 mL volume of 1,10-phenanthroline solution (5.5 mM), and the spectrum was recorded after the solution was left for a few minutes to develop. A third 1.0 mL aliquot was mixed with a 1.0 mL sample of sodium thiocyanate solution (10 mM), and the spectrum of the resulting solution was recorded. The net spectrum of the

thiocyanate solution after subtraction of the base line solution spectrum indicated no absorptions due to Fe(III) thiocyanate complexes; thus the ferric product found after exhaustive photolysis is not formed in the primary photolysis. In contrast, the net spectrum of the phenanthroline solutions showed strong absorptions characteristic of  $\text{Fe}(\text{phen})_3^{2+}$  ( $\lambda_{\text{max}} = 510 \text{ nm}$ ,  $\epsilon_{510} = 1.11 \times 10^4 \text{ M}^{-1} \text{ cm}^{-1}$ ), indicating the formation of ferrous products. RBS solutions which had not been photolyzed gave negative tests for both Fe(II) and Fe(III). By comparison of the absorbance changes seen during the photolysis to those recorded for the appropriate phenanthroline analytical tests, a product yield of  $3.8 \pm 0.3 \text{ mol}$  of Fe(II) per mole of **II** photodecomposed was determined for six separate experiments.

Nitrite and nitrate formation also draws support from electrospray mass spectrometric (EMS) analysis of the RBS solution after photolysis.<sup>29</sup> The EMS spectrum showed its largest peak at  $m/z$  46, consistent with  $\text{NO}_2^-$ , and another at much lower intensity at  $m/z$  62, consistent with the  $\text{NO}_3^-$ . Nitrite might be expected under aerobic conditions since  $\text{NO}_2^-$  is the principal product of NO autoxidation in aqueous solution.<sup>30</sup> At an intensity comparable to that of nitrate, an unidentified peak at  $m/z$  97 was observed. Notably, attempts to determine the EMS spectra of aqueous  $\text{Na}_2\text{S}$  and  $(\text{NH}_4)_2\text{S}$  also (inexplicably) gave the same  $m/z$  97 signal as the most intense peak.

Qualitative measurements using the modified CF microelectrodes as sensors clearly indicated that NO was released when an aqueous RBS solution was photolyzed at various  $\lambda_{\text{irr}}$  in an aerobic solution. This is consistent with earlier reports using biological assays (e.g., rat tail artery relaxation) to demonstrate release of NO upon RBS photolysis in buffered solutions.<sup>11,12</sup> Quantitative analyses were carried out using the combination electrode NO sensors. In those cases, broad band irradiation (360–440 nm band pass filter or the Pyrex and IR filtered output of a mercury arc lamp) was used to give light intensities sufficient to generate products quickly. Slow autoxidation in aerated solutions makes NO detection time dependent, so analysis and calibration must be carried out in a timely manner and under very analogous conditions. Figure 2 illustrates quantitative determination of the NO released upon irradiation of **II** in aerated pH 7.0 phosphate buffer solution. The solution absorption spectra were recorded before and immediately after photolysis. The signal from the NO sensor rose quickly when photolysis was initiated and then decreased slowly when the light was turned off (Figure 2 inset). The signals recorded upon photolysis were calibrated by generating comparable [NO] with standard solution aliquots. Quantum yields were not determined directly; instead the changes in  $[\text{II}]$  were evaluated quantitatively from the solution absorption spectra. From these data, the photolysis reaction stoichiometry ratio  $\Delta[\text{NO}]/\Delta[\text{II}]$  was cal-

(27) Sadtler Standard Grating Spectra, Sadtler Research Laboratories, Inc., 1974, v. 34: sodium nitrate spectrum, 33687; sodium nitrite spectrum, 33688.

(28) Metzler, D. E.; Myers, R. J. *J. Am. Chem. Soc.* **1950**, *72*, 3776–3780.

(29) The products of RRS photolysis were probed by using electrospray mass spectrometry. The EMS spectrum of an unphotolyzed aqueous RRS solution displayed a small peak at  $m/z$  148 for the nonhydrated dianion,  $\text{Fe}_2\text{S}_2(\text{NO})_4^{2-}$  plus stronger peaks at successive +9  $m/z$  values, consistent with different hydration numbers  $\text{Fe}_2\text{S}_2(\text{NO})_4^{2-x} \cdot x(\text{H}_2\text{O})$ , up to the  $x = 8$  which characterizes the solid. The most intense peak in the spectrum was at  $m/z$  236, probably  $\text{Fe}_2\text{S}_2(\text{NO})_2^-$ , followed by one at  $m/z$  266.5, possibly  $\text{Fe}_2\text{S}_2(\text{NO})_3^-$ . The EMS spectrum of a deaerated aqueous RRS solution after photolysis ( $\lambda_{\text{irr}} = 360\text{--}440 \text{ nm}$ ) to 70% conversion was more complicated. Samples were taken of the photolyzed solution under Ar and after exposure to air. (Notably, although the column is flushed with helium, it is not truly oxygen free.) In both, the black Roussinate anion **II** was evident, showing the same pattern of parent, NO-loss products, and waters of hydration as seen for the EMS spectrum of an aqueous RBS solution. A small nitrite peak at  $m/z$  46 appeared in both samples. Samples of the photolyzed solutions that were not exposed to air before being injected showed peaks at  $m/z$  354 and 324, assignable to  $\text{Fe}_3\text{S}_3(\text{NO})_3^-$  and  $\text{Fe}_3\text{S}_3(\text{NO})_2^-$ , respectively.

(30) Ford, P. C.; Wink, D. A.; Stanbury, D. M. *FEBS Lett.* **1993**, *326*, 1–3.

**Table 1.** Quantum Yields for Photoreactions of Roussin's Black Salt  $[\text{NH}_4][\text{Fe}_4\text{S}_3(\text{NO})_7]$  in Various Media

medium	$\lambda_{\text{irr}}$ (nm)	$\Phi_{\text{II}}^a$
H <sub>2</sub> O (aerobic) <sup>b</sup>	365	0.0011 ± 0.0001 (10)
H <sub>2</sub> O (deaerated)	365	<10 <sup>-6</sup> (2)
H <sub>2</sub> O (1.0 atm of O <sub>2</sub> )	365	0.0042 (1)
H <sub>2</sub> O <sup>b</sup>	313	0.0011 ± 0.0002 (2)
H <sub>2</sub> O <sup>b</sup>	436	0.0011 ± 0.0002 (2)
H <sub>2</sub> O <sup>b</sup>	546	~0.001 (1)
CH <sub>3</sub> OH (aerobic)	365	0.0021 ± 0.0001 (6)
CH <sub>3</sub> CN (aerobic)	365	0.0025 ± 0.0002 (3)
THF (aerobic)	365	0.0041 ± 0.0002 (3)

<sup>a</sup> In moles/einstein; number of independent determinations in parentheses. Experimental uncertainties represent average deviations from the mean value listed. <sup>b</sup> Unless otherwise noted, all aqueous solutions are aerobic pH 7.0 phosphate buffer solution at 0.22 M ionic strength.

culated to be about 6 ( $5.9 \pm 0.2$ , average of nine independent determinations).

**B. Quantum Yields for RBS Photolyses.** In independent experiments, quantum yields ( $\Phi_{\text{II}}$ ) for the disappearance of black salt anion  $\text{Fe}_4\text{S}_3(\text{NO})_7^-$  in aerated water were determined from optical density changes at different  $\lambda_{\text{mon}}$  (360, 374, and 420 nm). The spectral changes proved invariant with irradiation wavelength and gave the same  $\Phi_{\text{II}}$ ,  $0.0011 \pm 0.0001$  mol/einstein, for all  $\lambda_{\text{irr}}$  between 313 and 546 nm (Table 1). Thus, given the reaction stoichiometry determined above, the quantum yield for NO production  $\Phi_{\text{NO}}$  would be  $0.0065 \pm 0.0006$  in aerated aqueous solution.  $\Phi_{\text{II}}$  is markedly dependent on the dioxygen concentration and was found to be about 4-fold higher ( $\sim 0.0042$ ) under pure O<sub>2</sub> at 1.0 atm. On the other hand, in carefully deaerated solutions, absorbance changes were minimal upon photolysis, and the upper limit of  $\Phi_{\text{II}}$  was estimated as  $<10^{-6}$  mol/einstein under these conditions.

Quantum yields for RBS photolyses in several organic solvents under aerated conditions are also listed in Table 1. These  $\Phi_{\text{II}}$  values are somewhat higher than in water. The differences correlate qualitatively with the solubility of atmospheric O<sub>2</sub> in these solvents.<sup>31</sup>

The marked dependence of  $\Phi_{\text{II}}$  on the presence and (apparently) concentration of dioxygen in solution argues that O<sub>2</sub> serves to trap excited states or intermediates generated by initial excitation. In this context, it was decided to examine the photochemistry of deaerated aqueous RBS in the presence of a different oxidant. Among several possible oxidants examined (e.g.,  $\text{MnO}_4^-$  and  $\text{S}_2\text{O}_6^{2-}$ ), most gave thermal redox chemistry at rates inconvenient to use in the photochemical studies. However, dilute deaerated solutions of RBS (60  $\mu\text{M}$ ) plus  $\text{Co}(\text{NH}_3)_6^{3+}$  (1 mM as the chloride salt) only underwent a slow thermal reaction in the dark; thus they were sufficiently unreactive to probe the photochemistry. When such solutions were irradiated at 365 nm (where 89% of the light is absorbed by **II**), the systems demonstrated substantial photoactivity, with  $\Phi_{\text{II}}$  for the disappearance of **II** determined spectroscopically as 0.0021. This quantum yield increased as the Co(III) concentration was raised. Although the photolysis products were not further characterized, this experiment supports the view that a reactive intermediate (or an excited state) formed reversibly upon excitation of the substrate can be trapped by added oxidant.

The presence of a transient species formed by excitation of the black Roussinate anion **II** suggested by the chemical trapping experiments gains further credence from preliminary flash photolysis studies. Figure 3 illustrates the time-resolved optical

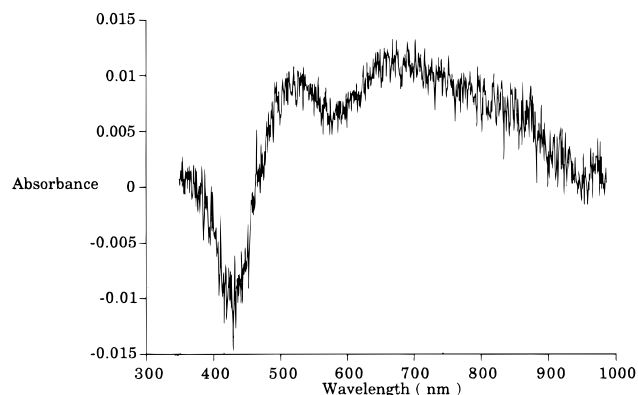


**Figure 3.** Transient (difference) spectrum seen in the flash photolysis of RBS (45  $\mu\text{M}$ ) in aqueous solution after 355 nm excitation. Gate width: 500 ns. Gate delay: 15 ns.

spectrum observed when a 60  $\mu\text{M}$  deaerated aqueous RBS solution at ambient temperature was irradiated with 10 ns pulses from the third harmonic of a Nd:YAG laser. Although it was shown above that continuous photolysis using near UV-visible light leads to little net photochemistry in deaerated solutions, it is clear from Figure 3 that one or more transient species are formed by photolysis. The lifetime(s) of such species under this condition are too long ( $>5$  ms) to measure accurately with the current flash photolysis apparatus, so it is improbable that the transient is an electronic excited state. (In addition, qualitative observations using both PMT and eyeball detectors were not able to detect any visible emission from these solutions). Similar experiments carried out under different  $P_{\text{NO}}$  demonstrated the lifetime of the intermediate(s) to be sensitive to NO and revealed the presence of a complicated scenario for the transient spectroscopy. Two intermediates were indicated by the kinetic studies, one which reacted according to a pathway showing a first-order dependence on  $[\text{NO}]$  ( $k_{\text{no}} \sim 7 \times 10^7 \text{ M}^{-1} \text{ s}^{-1}$ ), to give (apparently) a second intermediate, which eventually reacted to regenerate **II** over a period of milliseconds. Additional, more detailed studies of this transient behavior under different conditions are in progress.<sup>32</sup>

**Photoreactions of Roussin's Red Salt.** Although RRS solutions are less strongly colored than those of the black salt, the electronic spectrum of the red Roussinate anion **I** does show a strong transition centered at 374 nm ( $1.04 \times 10^4 \text{ M}^{-1} \text{ cm}^{-1}$ ), which tails well into the visible ( $\epsilon = 530 \text{ M}^{-1} \text{ cm}^{-1}$  at 550 nm) (Figure 1). EHMO calculations<sup>25</sup> indicate that the frontier orbitals of  $\text{Fe}_2\text{S}_2(\text{NO})_4^{2-}$  are largely composed of the iron AOs, the HOMO being metal-metal bonding, the LUMO metal-metal antibonding; thus the near UV-visible absorption bands would appear to be largely concerned with transitions between MOs delocalized over the two Fe atoms. That study<sup>24</sup> did not report details regarding contributions of nitrosyl orbitals, but if analogy to the black anion **II** carries over, it would appear likely that the LUMO of **I** has Fe-NO antibonding character as well.<sup>25</sup>

Aerated aqueous solutions buffered at pH 7.0 undergo slow thermal reaction (297 K) to give spectra consistent with  $\sim 10\%$  conversion of **I** to **II** within 2 h, but deoxygenated solutions were thermally stable for several days. At pH  $> 10$ , even aerated solutions are thermally stable, but at pH  $< 5$ , **I** undergoes rapid decomposition to unidentified species.

Photolysis of aqueous RRS solutions under either aerated or deaerated conditions results in quantitative conversion of **I** to **II** as evidenced by changes in the absorption spectra. The photoreaction appears to be stoichiometric, with isosbestic points appearing at 280, 312, and 424 nm (e.g., Figure 4). Since **I** is

(31) Battino, R., Ed. *Oxygen and Ozone: Solubility Data Series*; Pergamon Press: New York, 1981; Vol. 7.

(32) J. Bourassa, studies in progress.

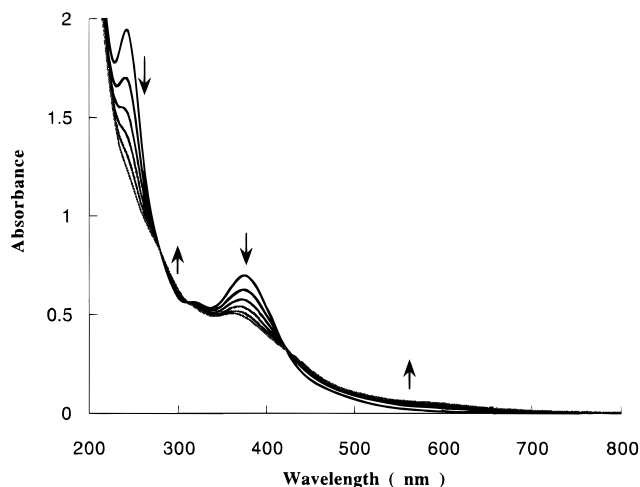


**Figure 4.** Photolysis of RRS solution ( $67 \mu\text{M}$ ) ( $\lambda_{\text{irr}}$  365 nm, 1 min intervals shown) showing isosbestic points and formation of **II**.

**Table 2.** Quantum Yields for Photoreactions of Roussin's Red Salt  $\text{Na}_2[\text{Fe}_2\text{S}_2(\text{NO})_4]$  in Various Media

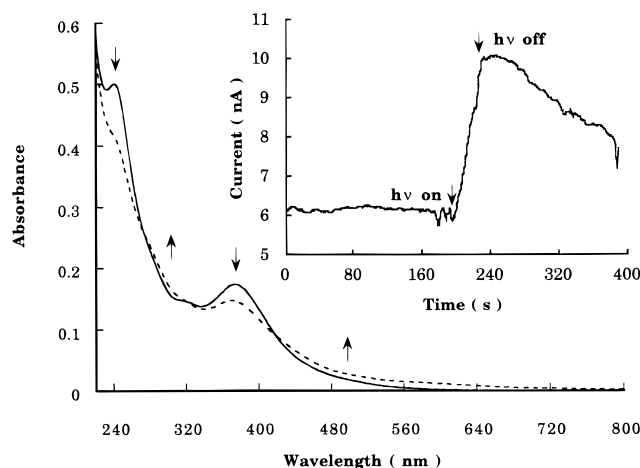
medium	$\lambda_{\text{irr}}$ (nm)	$\Phi_{\text{I}}^a$
$\text{H}_2\text{O}^b$	313	$0.142 \pm 0.006$ (8)
$\text{H}_2\text{O}$ (pH 7)	365	$0.138 \pm 0.006$ (6)
$\text{H}_2\text{O}$ (pH 7, deaerated)	365	$0.0039 \pm 0.0006$ (3)
$\text{H}_2\text{O}$ (pH 6)	365	$0.140 \pm 0.006$ (3)
$\text{H}_2\text{O}$ (pH 8)	365	$0.138 \pm 0.006$ (3)
$\text{H}_2\text{O}$ (pH 9)	365	$0.12 \pm 0.01$ (3)
$\text{H}_2\text{O}$ (pH 10)	365	$0.089 \pm 0.007$ (3)
$\text{H}_2\text{O}$	404	$0.135 \pm 0.006$ (2)
$\text{H}_2\text{O}$	436	$0.138 \pm 0.006$ (2)
$\text{H}_2\text{O}$	546	$\sim 0.13$ (1)
DMSO	365	$0.20 \pm 0.02$ (3)
MeCN	365	$0.30 \pm 0.02$ (3)
MeCN (deaerated)		$0.0047 \pm 0.0006$ (2)
$\text{Me}_2\text{CO}$	365	$0.39 \pm 0.01$ (3)
MeOH	365	$0.37 \pm 0.01$ (2)
MeOH (deaerated)		$0.012 \pm 0.001$ (2)

<sup>a</sup> In moles/einstein; number of independent determinations in parentheses. Experimental uncertainties represent average deviations from the mean value listed. <sup>b</sup> Unless otherwise noted, all aqueous solutions are aerobic pH 7.0 phosphate buffer solution at ionic strength = 0.22.

much more photoactive than **II**, interference from the secondary photolysis of the latter is minor. The formation of  $\text{Fe}_4\text{S}_3(\text{NO})_7^-$  was confirmed by electrospray mass spectrometry which displayed the pattern of parent, NO-loss products, and waters of hydration as seen for the EMS spectrum of an aqueous RBS solution.<sup>29</sup>

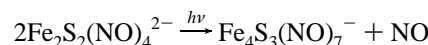
Quantum yields for the disappearance of **I** ( $\Phi_{\text{I}}$ ) were determined from the spectral changes under various aqueous solution conditions and in several different solvents (Table 2). Two key points are that  $\Phi_{\text{I}}$  displays little dependence on  $\lambda_{\text{irr}}$  and that it is  $\sim 50$  fold higher in aerated media ( $\Phi_{\text{I}} = 0.138$  for 365 nm irradiation in pH 7 buffered solutions) than under deaerated conditions (0.0039). In addition,  $\Phi_{\text{I}}$  values are modestly pH dependent and fall off at higher pH (Table 2). At pH > 11, photolysis of RRS solution results in formation of unidentified products. It was not possible to explore the quantum yield dependence on [NO] since **I** degrades thermally to unidentified species under NO.

Figure 5 illustrates the experiment to determine the reaction stoichiometry with regard to nitric oxide in the photolysis of aerated aqueous RRS solutions. In such photolysis experiments, the [NO] was determined electrochemically via *in situ* measurements with the combination electrode NO sensors,<sup>20</sup> and change in [I] was determined from the solution spectra. These



**Figure 5.** Absorption change amperogram of NO released upon 365 nm photolysis of an aerated pH 7.0 phosphate buffered solution of Roussin's red salt. WPI NO sensor used with calibrated sensitivity  $0.80 \text{ nA}/\mu\text{M}$ : initial [I] =  $15 \mu\text{M}$ ;  $\Delta[\text{I}]$  from spectral changes =  $-9.8 \mu\text{M}$ ;  $\Delta[\text{NO}]$  determined electrochemically =  $5.1 \mu\text{M}$ .

experiments demonstrated the stoichiometric ratio  $\Delta[\text{NO}]/\Delta[\text{I}]$  to be  $0.50 \pm 0.02$  (five independent experiments); i.e., the partial reaction stoichiometry is



By comparison to measured values of  $\Phi_{\text{I}}$ , the quantum yield for NO formation  $\Phi_{\text{NO}}$  can be calculated to be 0.069 under these conditions.

The head space of the photolysis cell above solutions of RRS after photolysis in deoxygenated conditions was sampled via syringe techniques in order to probe the nature of possible volatile products. GC analysis of these gases indicated the formation of some nitrous oxide ( $\text{N}_2\text{O}$ ) in significant excess of background; however, the amounts were not quantified.

Preliminary laser flash photolysis experiments in aerated solutions demonstrated formation of transient species that decayed via several sequential steps.<sup>32</sup> The instability of **I** under NO prevented examination of the decay kinetics as a function of solution [NO].

**Cell Culture Experiments.** Samples of RRS and of RBS were examined at the Bethesda laboratory for biological activity. Hypoxic cell cultures of Chinese hamster V79 cells were plated, infused with a solution of the appropriate compound at given concentrations, and exposed to visible light, to  $\gamma$ -radiation, to both sequentially or simultaneously, or to neither. The cells were plated and allowed to develop for 1 week, and the colonies which grew from viable cells were counted. By comparing these populations to appropriate controls, surviving fractions of the hypoxic cells were compiled to determine the effect of the salts as thermally biostatic compounds, phototoxic agents, or  $\gamma$ -radiation sensitizers. Appropriate control experiments were carried out simultaneously to ensure that the effects noted did not represent anomalies in handling of the cell cultures, and the survival fractions described for the various cytotoxicity, photosensitization, radiation, and radiosensitization experiments are all normalized against these controls. However, the resulting corrections are minor since the controls generally demonstrated survival fractions very close to 1.0 for hypoxic cells not subjected to other chemical or physical stress. In contrast, hypoxic cell suspensions subjected to a 15 Gy dose of  $^{60}\text{Co}$   $\gamma$ -radiation gave surviving fractions of 0.30, while aerobic cells treated similarly gave a value of  $<10^{-3}$ . The latter value illustrates the importance of oxygen to radiation treatment.

The black salt proved to be quite cytotoxic and showed strong growth inhibition of cell cultures even without  $\gamma$ -radiation or visible light treatment. Concentrations as low as 200  $\mu\text{M}$  resulted in the complete suppression of cell growth, and for this reason, radiosensitization experiments with RBS were not further pursued. RRS proved to be much less biostatic, with survival fractions of 0.63 for treatment with 1 mM RRS solution, >0.91 for treatment with 500  $\mu\text{M}$  RRS solution, and  $\sim 1.0$  for treatment with 100  $\mu\text{M}$  RRS solution under hypoxic conditions. However, it was noted that samples of RRS, which had been left as solids for some months since recrystallization, were considerably more toxic, presumably as the result of a slow degradation of **I** to **II** in the solid. Furthermore, treatment with 10 mM RRS solution proved to be quite toxic; the cells were noticeably stained, and the survival fraction was  $\sim 10^{-5}$ .

In general, broad band visible light irradiation of hypoxic V79 cells which were treated with the lower concentration RRS solutions ( $\leq 1$  mM) or were untreated had but small or no effect on the survival rates of viable cells. Thus there appears to be no simple photosensitization of cell mortality by visible light irradiation of RRS alone (a process termed "photodynamic therapy" or PDT, in cancer chemotherapy).<sup>33</sup> Separate control experiments were carried out to compare the effect of a 15 Gy dose of <sup>60</sup>Co radiation on hypoxic cells which had been similarly treated with RRS solutions to those which had not been treated, i.e., to determine RRS sensitization of  $\gamma$ -radiation.  $\gamma$ -radiation of untreated hypoxic cells and those which been treated with a 1 mM RRS solution gave the respective survival fractions 0.30 and 0.071, suggesting about 4-fold enhancement of radiation-induced damage resulting from this level of RRS. However, this concentration of RRS is already somewhat toxic (see above), so correction for normal cytotoxicity gives a lower net radiosensitization. Even this effect fell off significantly for slightly lower RRS concentrations (see below for experiments at 750  $\mu\text{M}$ ), so, like cytotoxicity, radiosensitization by RRS has a distinctly nonlinear character in these concentration ranges. On the other hand, simultaneous exposure of the 1 mM RRS solution treated cells with both light and  $\gamma$ -radiation led to a survival fraction of 0.0030. This suggests a synergism between RRS photoactivation and radiation damage to the cell cultures.

Figure 6 shows the survival of V79 cells exposed to varying doses of  $\gamma$ -radiation under hypoxic conditions. The dashed line on the plot indicates the response of V79 cells exposed to  $\gamma$ -radiation under fully aerobic conditions, and comparison with the control serves to demonstrate further the resistance of hypoxic cells (open circles) to radiation. RRS solution treatment alone at this concentration (750  $\mu\text{M}$ ) resulted in little cytotoxicity. Cells treated with Roussin's red salt but receiving no light treatment showed minimal radiosensitization (Figure 6, open squares) at lower doses, and perhaps even some radiation protection at the higher doses. On the other hand, analogously RRS treated cells exposed simultaneously to white light and  $\gamma$ -radiation were significantly radiosensitized (closed circles).<sup>34</sup> White light illumination alone did not alter the radiation response or hypoxic cells (data not shown). Furthermore, hypoxic cells first treated with such RRS solutions, illuminated with visible light, and then subjected to  $\gamma$ -radiation in a sequential fashion showed no difference in survival rates from those cells where the visible light step was eliminated (data not shown). Thus, it

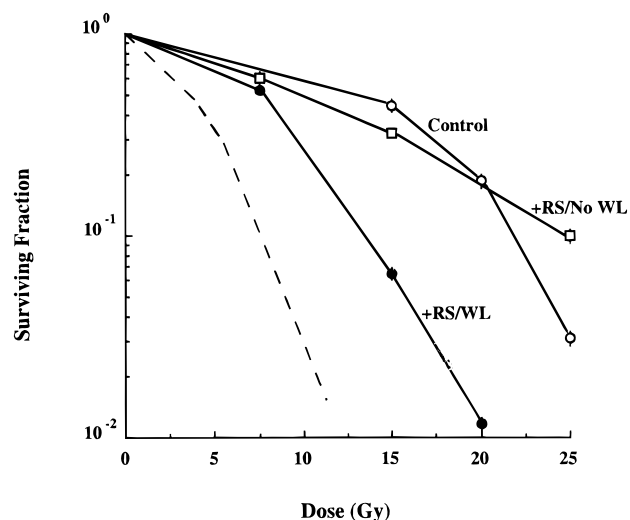


**Figure 6.** Survival of V79 cells exposed to  $\gamma$ -radiation under hypoxic conditions in the absence (open circles) or presence of 500  $\mu\text{M}$  Roussin's red salt with (closed circles) or without (open squares) light exposure. The dashed line on the plot indicates the response of V79 cells exposed to  $\gamma$ -radiation under fully aerobic conditions (ref 23). (WL refers to white light illumination; see Experimental Section.)

is clear that the photochemical radiosensitization of these hypoxic cells requires simultaneous treatment with light and radiation.

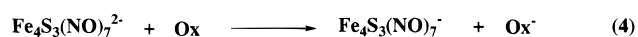
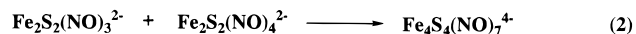
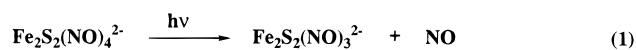
## Discussion

The present work establishes unequivocally that the photochemical reactions of the Roussinate anions **I** and **II** generate nitric oxide as a key photoproduct. In principle, therefore, these two species can be used as precursors in photochemical strategies to deliver NO to biological targets. The photochemical delivery of NO under biologically relevant conditions was indeed realized in the cell culture tests described here, where it was shown that simultaneous visible light illumination of cells which had been treated with Roussin's red salt served to sensitize the  $\gamma$ -radiation induced cell mortalities. This sensitization can be attributed to photochemical delivery of NO simultaneous with the radiation treatment, consistent with prior observations that NO delivered by thermochemical reactions of precursors is a radiation sensitizer in cell culture tests. Furthermore, there was little sensitization in cases where the RRS treated cells were not illuminated or had been illuminated only during a period prior to initiating radiation treatment, so radiosensitization can be attributed to a relatively short-lived photoproduct in the system such as NO, not to RRS itself or a permanent photoproduct. The sensitizer role of NO apparently is based on its ability to intercept radiation-generated carbon-centered radicals,<sup>7</sup> thereby fixing the damage to and inhibiting repair of the target molecules, i.e., DNA. Although previous workers have reported that RBS could be used as a photochemical or thermal source of NO in various tissues, the present studies have found that RBS is quite toxic to the V79 cell cultures.

The photoreactions of transition metal complexes often reflect the nature of the lowest energy excited states (LEES) owing to rapid relaxation from higher energy states to the LEES. One indicator of such behavior is the quantum yield's independence of  $\lambda_{\text{irr}}$ , as is the case for  $\Phi_{\text{I}}$  and  $\Phi_{\text{II}}$ . For  $\text{Fe}_4\text{S}_3(\text{NO})_7^-$ , the nature of the LEES is not clear; however, the EHMO calculations noted above indicate that the LUMO of **II** has antibonding character with regard to Fe-Fe interactions and to Fe-S and Fe-NO bonds. Similar properties might reasonably be attributed to the frontier orbitals of  $\text{Fe}_2\text{S}_2(\text{NO})_4^{2-}$ . Thus the LEES

(33) Dougherty, T. S. *Photochem. Photobiol.* **1987**, *45*, 879-889.

(34) Another way to evaluate the effectiveness of the sensitizer is to use sensitizer enhancement ratios (SERs). SERs are calculated by dividing the radiation dose for control hypoxic conditions by the radiation dose for various agents or alternative procedures under hypoxic conditions at the 10% surviving fraction level (ref 23). The experiments with 0.75 mM RRS (Figure 6) gave a SER of  $\sim 1.6$ .

**Scheme 1**

would appear to have significantly weakened bonds sustaining the  $\text{Fe}_x\text{S}_y$  cluster core as well as weakened Fe–NO interactions. In this context, one might expect cluster fragmentation or NO dissociation to accompany photoexcitation. However, the complex sequence of events required for transformation of the diiron red Roussinate **I** to the tetrairon black Roussinate **II** as well as the total decomposition of **II** to ferric salts is far from being elucidated in the present case. What is clear is that, for both species, bimolecular processes with an external oxidant to trap the transients formed in initial photoexcitation steps play a major role in effecting the net photoreaction. This is an absolute requirement in the photolysis of the black anion **II** in solution (no net photochemistry is seen in the absence of such trapping agents) and has a major impact on the efficiency of the transformation of **I** to **II**.

Scheme 1 illustrates a speculative model for the photochemistry of **I** in aqueous solution consistent with the reaction stoichiometry. In the absence of oxygen or another oxidant, it is possible that NO would act as an oxidant. Electrochemical studies show that the reduction potential of  $\text{Fe}_4\text{S}_3(\text{NO})_7^-$  is  $-0.44$  V while the reduction potential for NO is  $-0.33$  V<sup>35</sup> (both vs NHE) in aqueous solution, so the  $\Delta E$  for eq 4 in Scheme 1 is favorable for Ox = NO (0.11 V). If this were the case, then nitroxyl anion  $\text{NO}^-$  would be a product. Protonation of  $\text{NO}^-$  and dimerization would give  $\text{N}_2\text{O}_2\text{H}_2$ , which is the

(35) (a) Crayston, J. A.; Glidewell, C.; Lambert, R. J. *Polyhedron* **1990**, *9*, 1741–1746. (b) Stanbury, D. M. *Adv. Inorg. Chem.* **1989**, *33*, 69–135.

hydrate of  $\text{N}_2\text{O}$ , a species observed qualitatively as a photo-product of photolysis under deaerated conditions. This would be consistent with Scheme 1, but observation of  $\text{N}_2\text{O}$  does not constitute proof of nitroxyl formation. It is hoped that ongoing studies of the reaction kinetics of intermediates formed by laser flash photolysis of these systems will better elucidate mechanistic aspects of the photoreactions of both the red and black Roussinate anions.

**Summary**

The following key points should be emphasized:

(1) The photochemical reactions of the red and black Roussinate anions have been examined quantitatively, and it has been established that in aerated solutions both can serve as photochemical precursors of NO.

(2) RRS solutions are several orders of magnitude more photoactive than are analogous RBS solutions, and both are much more active under aerated rather than deaerated conditions. This can be attributed to the necessity for an oxidant to be present in order to intercept key intermediates before reassembly of these to the original clusters. The RRS anion **I** photochemically undergoes transformation to **II**, while the less efficient aerobic photoreaction of the latter leads eventually to complete decomposition of the cluster to Fe(III), NO, sulfur, and other unknown products via the intermediacy of ferrous species.

(3) The photoactivity of RRS solutions was exploited to demonstrate the viability of the proposed strategy to deliver NO to biological targets. In this case, NO generated photochemically was used to sensitize the  $\gamma$ -radiation induced mortalities of hypoxic V79 cell cultures. The black salt proved toxic to the V79 cell cultures and was not studied further in this context.

**Acknowledgment.** Studies at UCSB were supported by the National Science Foundation (CHE 9400919). The Roussinate salts were first brought to our attention by Dr. Peter Kovacic.

JA963914N